Lacoux et al. Supplementary data

MATERIALS and METHODS

DNA primers used for the primer extension analysis (assay at low dNTP concentration)

BMN155: 5'-GAGCTGAGGACCGAACCCAGG- 3'

BMN297: 5'-CCAGAGCTGAGGACCG- 3'

U2 snRNA:

U2.2: 5'-CAAAAATCCATTTAATATAT-3'

Construction of *U1* RNA

U1 snRNA:

U1-5' T7: 5'-ATATAATACGACTCACTATAGGATACTTACCTGGCAGGG-3'

U1-3': 5'-CAGGGGAAAGCGCGAACGCAG-3'

RNA primers used to reconstitute *BC1* RNA and for the EMSA assays

Unmethylated *BC1* 5' hairpin:

5'-UGGGGAUUUAGCUCAGUGGUAGAGCGC

UUGCCUAGCAAGCGCAAGGCCCUGGGUUCGGUCCUCA-3'

2'*O*-Methyl *BC1* 5' hairpin:

5'-UGGGGAUUUAGCUCAGUGGUAGAGCGCUUG

CCUAGCAAGCmGmCAAGGCCCUmGGGUUCGGUCCUCA-3'

BC1 3'end:

BC1 3'SP6: 5'-GATTTAGGTGACACTATAGCTCTGGAAAAAAAAAA-3'

BC1 3': 5'-AAAGGTTGTGTGTGCCAGTTA-3'

Splint DNA oligo:

5'-TTTTTTTTTTTCCAGAACCGAACCCAGGGCCTT'-3'

BC1 RNA oligos have been purchased from Dharmacon; *BC1* DNA oligos from Eurofins MWG operon.

Primer Labelling

Each primer was [32P] γATP labelled according to the standard procedures. Radiolabelled primers were purified on BioRad Spin 6 columns according to the manufacturer's instructions.

***In vitro* transcription**

Sense *BC1* and *U2* RNAs were generated using the T7-directed *in vitro* transcription (MegaScriptT7 kit, Ambion) and pBCX607 (gift of H.Tiedge) and pT7U2 (gifts of T.Kiss) plasmids respectively.

For the sense *U1*, the human *U1* gene was amplified using the plasmid phU1 (gift of T. Kiss) and the U1 5'T7 and U1 3' primers. The PCR product was used as template to transcribe full length *U1* sense (MegaScriptT7 kit, Ambion). For the 3' hairpin *BC1* transcripts, the *BC1* 3'end was amplified using the pBCX607. Transcripts were purified on 8 M urea-8% acrylamide gels.

RNA isolation

RNA from total brain tissue was extracted with Trizol (Invitrogen) and separated on an 8 M urea/8% acrylamide gel. The band corresponding to *BC1* RNA was visualized by UV shadowing, excised, eluted overnight in 200 μl elution buffer (500mM NaOAc pH 5.3, 1 mM EDTA), extracted with phenol-chloroform isoamyl alcohol, and precipitated using absolute ethanol and glycogen. RNA was pelleted and washed using 70% EtOH and dried. RNA enriched for BC1 was purified by gel electrophoresis using *in vitro* synthesized *BC1* RNA as a marker. After purification, the identity of the RNA was confirmed by Northern blotting using the radiolabelled CD22 DNA primer.

Reconstruction of *BC1* RNA

The modified or unmodified 5' hairpin was aligned to the 3' hairpin using an oligo DNA splint and ligated in the presence of T4 RNA ligase as previously described (1). The final product was visualized on an 8 M-urea/10% acrylamide gel and the corresponding band cut, eluted and radiolabelled as described before.

RT-qPCR (SYBR-Green and TaqMan)

For total brain cytoplasmic extracts (WT and *BC1* KO) equal volume from each polysomal fraction was extracted and the RNA was reverse transcribed by MoMLV reverse transcriptase (Invitrogen). RT-qPCR analysis of polysomal gradients from WT and *BC1* KO brain was performed using the TaqMan (Applied Biosystems) system while from synaptosomal extracts using a LightCycler480 (Roche).

For the ABI 7900 Sequence Detector with dual-labeled TaqMan probes (Applied Biosystems) mouse *Arc* mRNA was detected with Pre-Developed TaqMan probe Mm00479619_g1 which generates a 71-bp amplicon from the NM_018790.2 sequence; mouse *Map1B* mRNA was detected with Pre-Developed TaqMan probe Mm00485261_m1 which generates a 87-bp amplicon from the NM_008634.1 sequence; and mouse α*CaMKII* mRNA was detected with Pre-Developed TaqMan probe Mm00437967_m1 which generates a 83-bp amplicon from the NM_177407.2 sequence. The relative amount of *Arc*, *Map1B* and α*CaMKII* mRNAs was assessed by comparison with the mouse *H3f3b* (H3 histone family 3b) mRNA detected with the Pre-Developed TaqMan probe Mm00787223_s1 (endogenous control), which generates an amplicon of 82 bp from the NM_008211.2 transcript. Final reaction volume was 20 μl in TaqMan Universal PCR Master Mix (ABI 4304437). Cycle parameters were 2 min at 50°C and 10 min at 95°C, followed by 40 cycles of 15 sec at 95°C for denaturation and 1 min at 60°C for annealing/extension. Relative *Arc*, *Map1B* and α*CaMKII* mRNA levels on polysomes (PMP ratio), normalized to *H3f3b*, were calculated as follows: $(2^{(-deltaCtP)}/(2^{(-deltaCtP)} + 2^{(-deltaCtNP)})*100$, where deltaCtP and deltaCtNP are the Cts of the Polysomal and Non Polysomal fractions, respectively of α*CamKII*, *Map1B* and *Arc* normalized for *H3f3b*.

For the LightCycler480 (Roche) each RT-qPCR reaction was performed in 15μl final volume with the LightCycler480 SYBRGreen I Master. The cycle parameters were: 10 min at 95°C as pre-amplification step; 20 sec at 95°C; 15 sec at 60°C; 15 sec at 72°C for 40 cycles as amplification step; and warming from 60°C to 95°C for the melting curve. The specificity of each RT-PCR reaction was confirmed by a melting curve analysis. In all cases, only one

peak was observed between 70-80°C, that depended on the length of the amplified fragment. The level of each mRNA on polysomes was calculated as follows: $(Eff^{(-deltaCtP)}/(Eff^{(-deltaCtP)} + Eff^{(-deltaCtNP)})*100$, where deltaCtP and deltaCtNP are the Cts of the Polysomal and Non Polysomal fractions respectively. Eff is the efficiency of the amplification calculated performing the PCR on 5 dilutions (with a factor of 2 or 4 between each dilution) of a reverse transcription reaction performed with 400ng of synaptic RNA in 20 µl reaction volume and fit to a logarithmic function. The efficiency ranged between 1.8 and 2.0. Each mRNA was normalized for *rRNA18S* (synaptoneurosomes) or *H3f3b* (total brain).

Primers used for RT-qPCR

αCaMKII: Forward (qCB5): 5'-CGGACATCTATGTGATAACTAGACC-3'; Reverse (qCB6): 5'-CACTTCCCAACCCATCCGA-3'

Map1b: Forward (qCB9): 5'-CTTCCGCTCCTCAATGCTA-3'; Reverse (qCB10): 5'-CGCTGTCTTTCTCCACACT-3'

Arc: Forward (qCB21): 5'-CTACAGAGCCAGGAGAATGAC-3'; Reverse (qCB22): 5'-TTTCCAGACATGGCAGCAAAGA-3'

rRNA 18S: Forward (qCB41): TGCGGCTTAATTTGACTCAACA; Reverse (qCB42): CGAGAAAGAGCTATCAATCTG

Western blot analysis

Protein analysis was performed as previously described (2). In this case 5 µg of total and synaptic proteins were analyzed. Synaptic preparations were evaluated by the presence of synaptic APP (3) and enrichment of the postsynaptic protein PSD-95 (4). For quantitative western blot, chemilumescence signal was acquired using the Fujifilm LAS3000 and further quantified using the Image Quant software (GE Healthcare) or AIDA software (Raytest Isotopenmeßgeräte GmbH). Western blotting was performed following standard procedures, using precast 18-well 4-12% Bis-Tris CriterionXT gels from BioRad, run in 1X MOPS. Antibodies used: GAPDH (Chemicon 1:10000); αCaMKII (Chemicon 1:1000); MAP1B (1:30000 kindly provided by Gary Bassell), Arc (Synaptic System 1:2000); PSD-95 (BD

Transduction Labs 1:1000); APP (Sigma 1:5000); FMRP (1:500) (5); Dyskerin (1:1000, kindly provided by Yves Henry) (6).

Synaptoneurosome preparation and RNA extraction

Synaptoneurosomes were prepared by homogenizing fresh cortex-hippocampus-striatum tissue in ice-cold buffer and processed through a flotation Percoll gradient as previously described (2). The synaptoneurosomes were resuspended in 0.5 ml HEPES-Krebs buffer (20 mM HEPES pH 7.4, 147 mM NaCl, 3 mM KCl, 10 mM glucose, 2 mM MgSO4, 2 mM CaCl2), equilibrated at 37°C for 10 min, and then lysed for RNA and protein analysis.

Synaptosomal RNA was extracted using proteinase K. Briefly, synaptosomes were lysed in 0.2 M NaOAc pH 4.8, 0.5% SDS, and 1 mM EDTA; 0.2 mg/ml proteinase K was added and digestion continued for 30 min at 37°C. A phenol/$CHCl_3$ extraction was performed, followed by $CHCl_3$ extraction and precipitation in 2.5 vol EtOH at -80°C overnight with 10 μg of glycogen added as a carrier. RNA was quantified and evaluated with an ND-1000 spectrophotometer (NanoDrop Technologies) as well as by electrophoresis.

RT-PCR and RT-qPCR analysis

First-strand synthesis was performed using p(dN)6 and 100 U of M-MLV RTase (Invitrogen). PCR was performed as previously described (7) using specific oligonucleotides to amplify β-*Actin*, α*CaMKII, Arc* and *Map1B* using oligos described in Supplementary Information. Real Time PCR was performed using an ABI 7300 Sequence Detector with dual-labeled TaqMan probes (Applied Biosystems) using Pre-Developed TaqMan assays, as described above.

Sucrose gradient to separate polysomes and mRNPs

Each gradient was collected in 10 fractions followed by the addition of 1% SDS (final concentration), 80 pg of synthetic rp*L22* or 25 pg of synthetic *BC200* RNAs, 10 μg glycogen, and proteinase K (100 μg/ml) and incubated for 30 min at 37°C. The synthetic RNAs were used to normalize for possible RNA loss during RNA phenol/chloroform extraction and precipitation from each fraction. RNAs were precipitated with 0.2 M NaOAc pH 4.8 and 0.7

vol of isopropanol. The pellets were resuspended in 30 µl or 15 µl of ddH_2O for total brain or synaptosome respectively, and the RNA fractions 1-5 (polysomal fraction, P) and 6-10 (mRNP fraction, NP) were pooled and RNA quality/quantity was assessed by 1.8% agarose formaldehyde gel electrophoresis and spectrophotometry (ND-1000 spectrophotometer, Nanodrop Technology). mRNAs of interest were quantified by RT-qPCR (see below), and the percentage of mRNAs on polysomes (PMP) was calculated as the ratio of the mRNA in fraction P over the total of fractions P and NP; a higher value indicates that a higher portion of the mRNA was associated with ribosomes at the time of fractionation and thus engaged in translation.

Computational procedures

The program generates different fragments of RNA that are further iteratively assembled applying constraints on the basis of the 2D structure. One hundred 3D structures of *BC1* 5' end were generated and for each of them a steepest descent energy minimization has been performed in order to refine the model. The structure with the lowest free energy value was selected for the docking experiment. The protein-RNA molecular dockings were performed using the program HADDOCK, properly implemented for the prediction of protein-nucleic acids interactions (8). Two regions of the FMRP-NT domain revealed by cross-linking experiments were used for the *BC1* RNA docking simulations. For each of the 20 NMR structures present in the PDB file of the FMRP-NT domain (PDB code 2BKD), 20 runs of docking with the 3D structure *BC1* 5' end were carried out. The results were clustered based on the RMSD (Root Mean Square Deviation) criterion, using a cut-off of 4.5 Å. Docking simulations of WT, mutant R70E-R111E and mutant Y103-N104N generated nine, four and seven families respectively. For each docking simulation the cluster analysis was carried out. For the interaction analysis, the complex with the best HADDOCK score was selected from the most populated families of each docking simulations.

Currently no docking program is able to consider RNA 2'-*O*-methylations in the interaction prediction, so the best HADDOCK score has been evaluated for the WT (unmethylated) *BC1*

5' complexes and then two methyl groups on both G46 and C47 (Gm46/Cm47), have been added by molecular modelling. The methyl groups on the 2'-*O* atom of the ribose moieties, and the structural differences caused by the amino acid substitution were modelled using the Sybyl 6.0 program (http://www.tripos.com) and the resulting structures were manually checked for altered interactions. The analysis of hydrogen bonds and electrostatic interactions were performed with the WHAT IF (9) and VMD (10) programs, respectively.

FIGURE LEGENDS

Supplementary Figure 1. (**A**) Protein enrichment in synaptoneurosomes. Total (T) and synaptic (S) extracts were analyzed for APP, PSD-95 and GAPDH proteins. (**B**) RNA enrichment in synaptoneurosomes. α*CaMKII*, *H3.3* mRNAs and *BC1* RNA and were detected from Total (T) and Synaptic (S) RNA preparations using RT-qPCR**. (C)** Enrichment in cytoplasmic and nuclear proteins. Cytoplasmic and nuclear fractions were analyzed for the presence of Dyskerin and GAPDH proteins.

Supplementary Figure 2. (A) Left panel, 2'-*O*-methylation assays performed using a primer extension at low dNTPs. Low dNTP concentrations create a primer extension stop one nucleotide before the 2'-*O*-methylated nucleotide; the products of the extension are visualised on a denaturing sequencing gel. Right panel: detection of 2'-*O*-methylations in *U2* RNA (lanes 1-3), sequence of *U2* RNA (lanes 4-7). (**B**) Sequence of *BC1* RNA from nt 39 to nt 1 (lanes 1-4). In absence of modifications the primer extension reaction using synaptic RNAs and the BMN155 primer stops at nt 1 of *BC1* RNA, see asterisk (lanes 5-6).

Supplementary Figure 3. (**A**) Raw data generated from the EMSA (Fig. 3A) are shown as the plot of the ratio bound/unbound RNA against the concentration of the His-FMRP-NT (from 0.04 μM to 1 μM); linear line is explained as y=10.43x with R2=0.9989; the two last points do not fall on the line due to binding saturation. **(B)** Scheme of the T4 RNA ligase method used to reconstitute the entire *BC1* RNA (unmodified or 2'-*O*-methylated). *BC1* 5' hairpins are ligated to the *BC1* 3' hairpin using a Splint DNA linker (in red) in presence of T4 RNA ligase. The product of the ligase reaction is separated on an 8 M urea/10% acrylamide gel and purified. (**C**) *BC1* RNA 2'-O-methylation reduces its binding to FMRP. Left panel, short *BC1* RNA oligonucleotides (65 nt) used for the EMSA assays. Central panel, EMSA using WT FMRP-NT and 2'-*O*-methylated or unmodified *BC1* RNA oligonucleotides. FMRP-NT (375-1875 ng) was incubated with 500 fmol of radiolabelled unmodified (lanes 2-5) or 2'-*O*-methylated (lanes 7-10) *BC1* RNA oligonucleotides. Lanes 1 and 6 contained unbound

BC1 RNA. The FMRP-*BC1* RNA complex is indicated by an asterisk, the unbound oligonucleotide is denoted by brackets. Right panel, the histogram shows the ratio of the Kd (2'-*O*-methylated/unmodified). Error bars represent SE: **P*<0.05 for methylated versus unmodified, by Student's test, n=3.

Supplementary Figure 4. (**A**) Expression of the FMRP-NT mutants. FMRP-NT Y103A-N104A was expressed in *E.coli,* purified on Ni-Sepharose beads and visualized on SDS-PAGE gel. Lane 1: protein marker, lanes 2-3: protein elutions. (**B**) Same as in (**A**) for the FMRP-NT R70E-R111E. Lane 1: protein marker, lane 2: input, lanes 2-3: protein elutions.

Supplementary Figure 5. mRNAs associated to FMRP in total brain and at synapses. Left panel, FMRP was immunoprecipitated and *β-Actin*, *αCaMKII*, *Arc* and *Map1B* mRNAs were detected by RT-PCR. Lanes 1-3: total brain extracts. Lane 1: input (1/50), lane 2: FMRP IP, lane 3: IgG IP using 30 PCR cycles. Lane 4 to 6: same as in 1-3 using synaptoneurosomes extracts. Right panel, same as in left panel (lanes 1-3) using 35 PCR cycles.

Supplementary Table 1. Hydrogen bond and salt bridge network affecting FMRP-NT and *BC1* RNA interaction. Note that not all interactions occur simultaneously in the same modeling solution.

REFERENCES

1. Stark, M.R., Pleiss, J.A., Deras, M., Scaringe, S.A. and Rader, S.D. (2006) An RNA ligase-mediated method for the efficient creation of large, synthetic RNAs. *RNA*, **12**, 2014-2019.

2. Napoli, I., Mercaldo, V., Boyl, P.P., Eleuteri, B., Zalfa, F., De Rubeis, S., Di Marino, D., Mohr, E., Massimi, M., Falconi, M. *et al.* (2008) The fragile X syndrome protein represses activity-dependent translation through CYFIP1, a new 4E-BP. *Cell*, **134**, 1042-1054.

3. Hoe, H.S., Fu, Z., Makarova, A., Lee, J.Y., Lu, C., Feng, L., Pajoohesh-Ganji, A., Matsuoka, Y., Hyman, B.T., Ehlers, M.D. *et al.* (2009) The effects of amyloid precursor protein on postsynaptic composition and activity. *J Biol Chem*, **284**, 8495-8506.

4. Sheng, M. (2001) Molecular organization of the postsynaptic specialization. *Proc Natl Acad Sci U S A*, **98**, 7058-7061.

5. Ferrari, F., Mercaldo, V., Piccoli, G., Sala, C., Cannata, S., Achsel, T. and Bagni, C. (2007) The fragile X mental retardation protein-RNP granules show an mGluR-dependent localization in the post-synaptic spines. *Mol Cell Neurosci*, **34**, 343-354.

6. Hoareau-Aveilla, C., Bonoli, M., Caizergues-Ferrer, M. and Henry, Y. (2006) hNaf1 is required for accumulation of human box H/ACA snoRNPs, scaRNPs, and telomerase. *RNA*, **12**, 832-840.

7. Zalfa, F., Eleuteri, B., Dickson, K.S., Mercaldo, V., De Rubeis, S., di Penta, A., Tabolacci, E., Chiurazzi, P., Neri, G., Grant, S.G. *et al.* (2007) A new function for the fragile X mental retardation protein in regulation of PSD-95 mRNA stability. *Nat Neurosci*, **10**, 578-587.

8. Dominguez, C., Boelens, R. and Bonvin, A.M. (2003) HADDOCK: a protein-protein docking approach based on biochemical or biophysical information. *J Am Chem Soc*, **125**, 1731-1737.

9. Vriend, G. (1990) WHAT IF: a molecular modeling and drug design program. *J Mol Graph*, **8**, 52-56, 29.

10. Humphrey, W., Dalke, A. and Schulten, K. (1996) VMD: visual molecular dynamics. *J Mol Graph*, **14**, 33-38, 27-38.

Supplementary Fig. 1

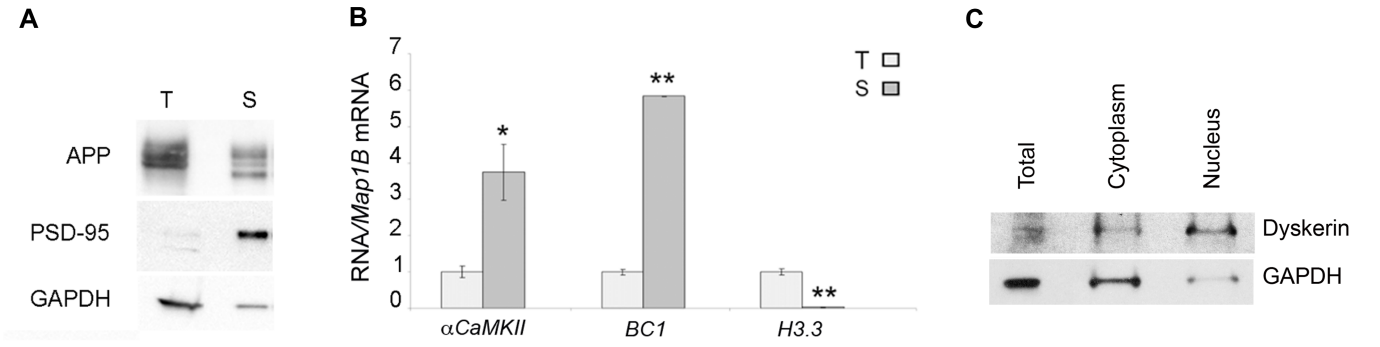

Supplementary Fig. 2

A

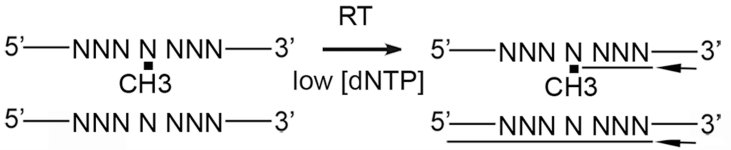

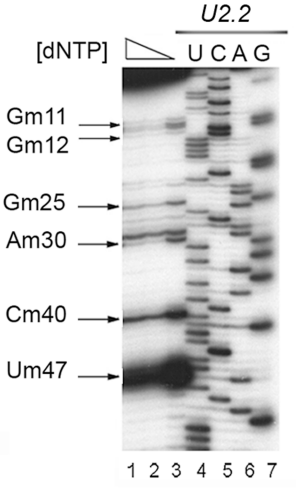

B

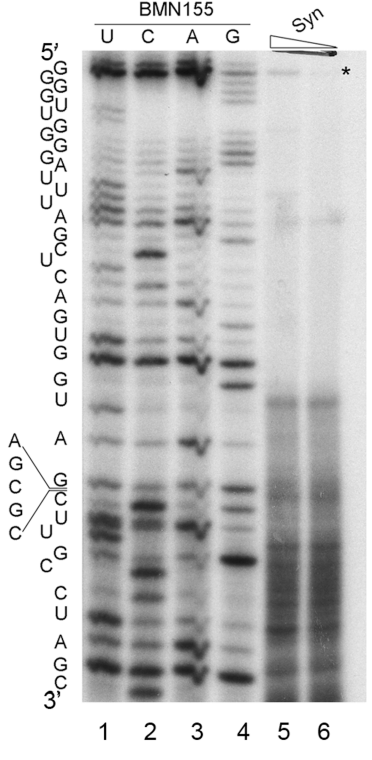

Supplementary Figure 3

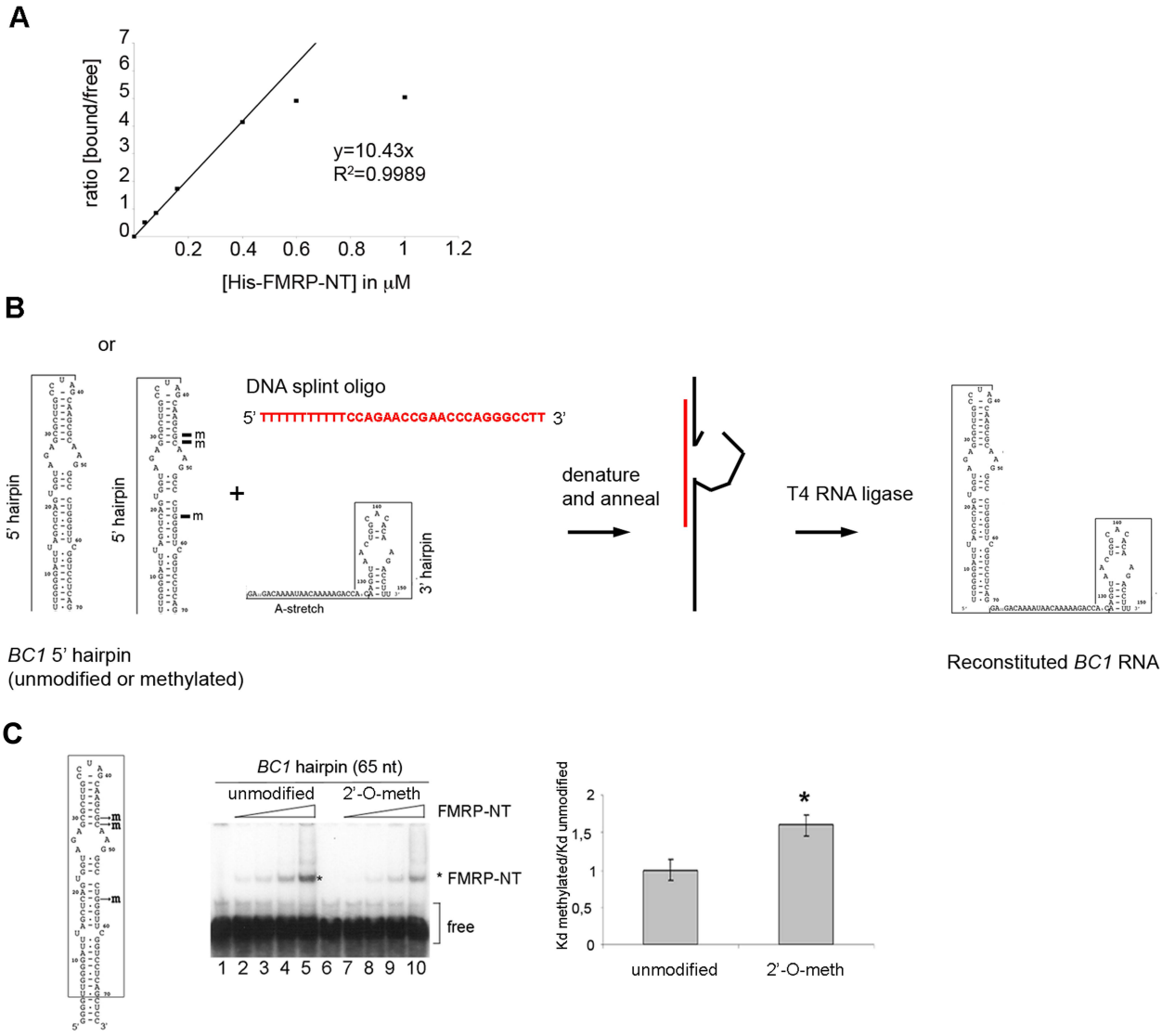

Supplementary Fig. 4

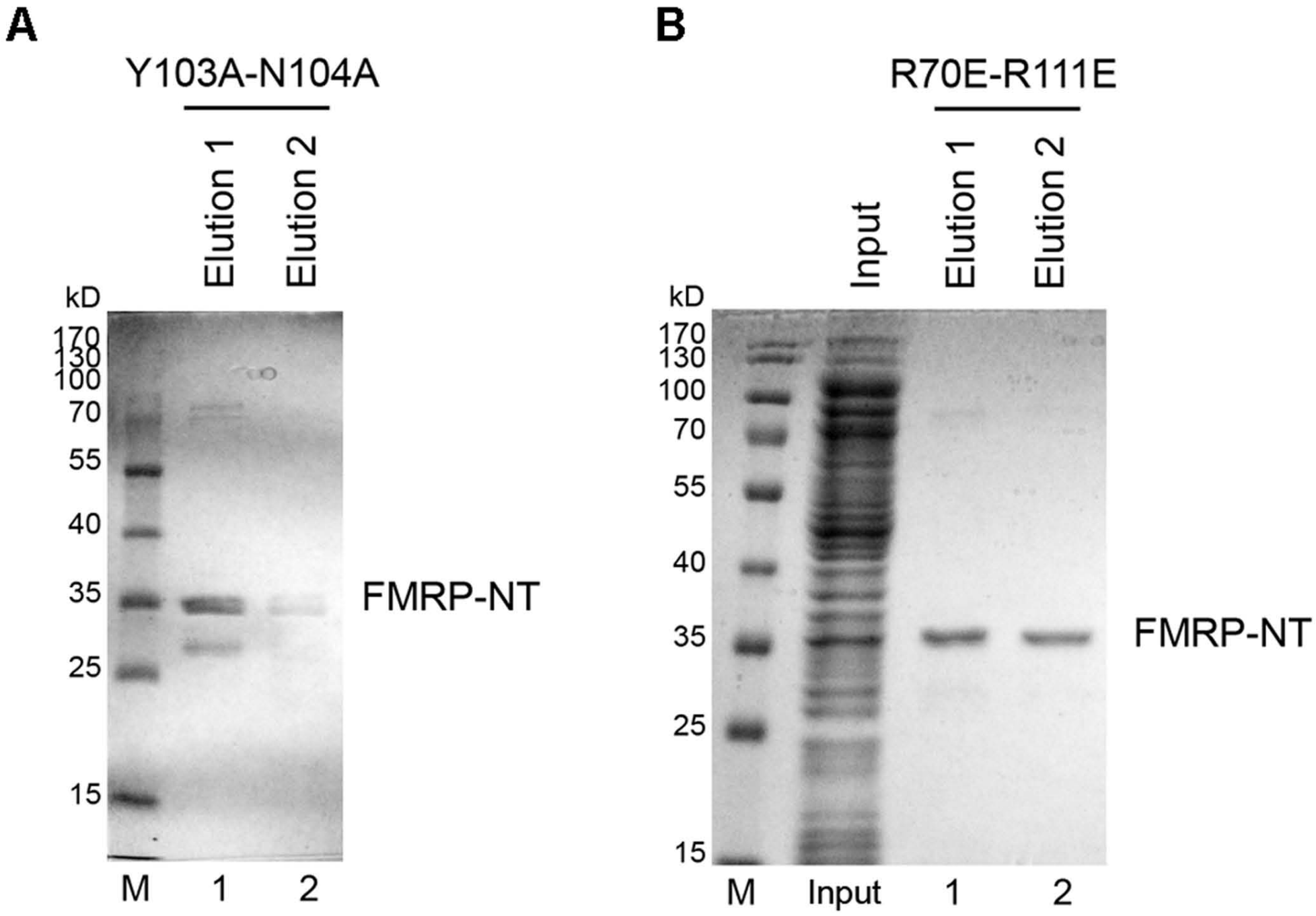

Supplementary Fig. 5

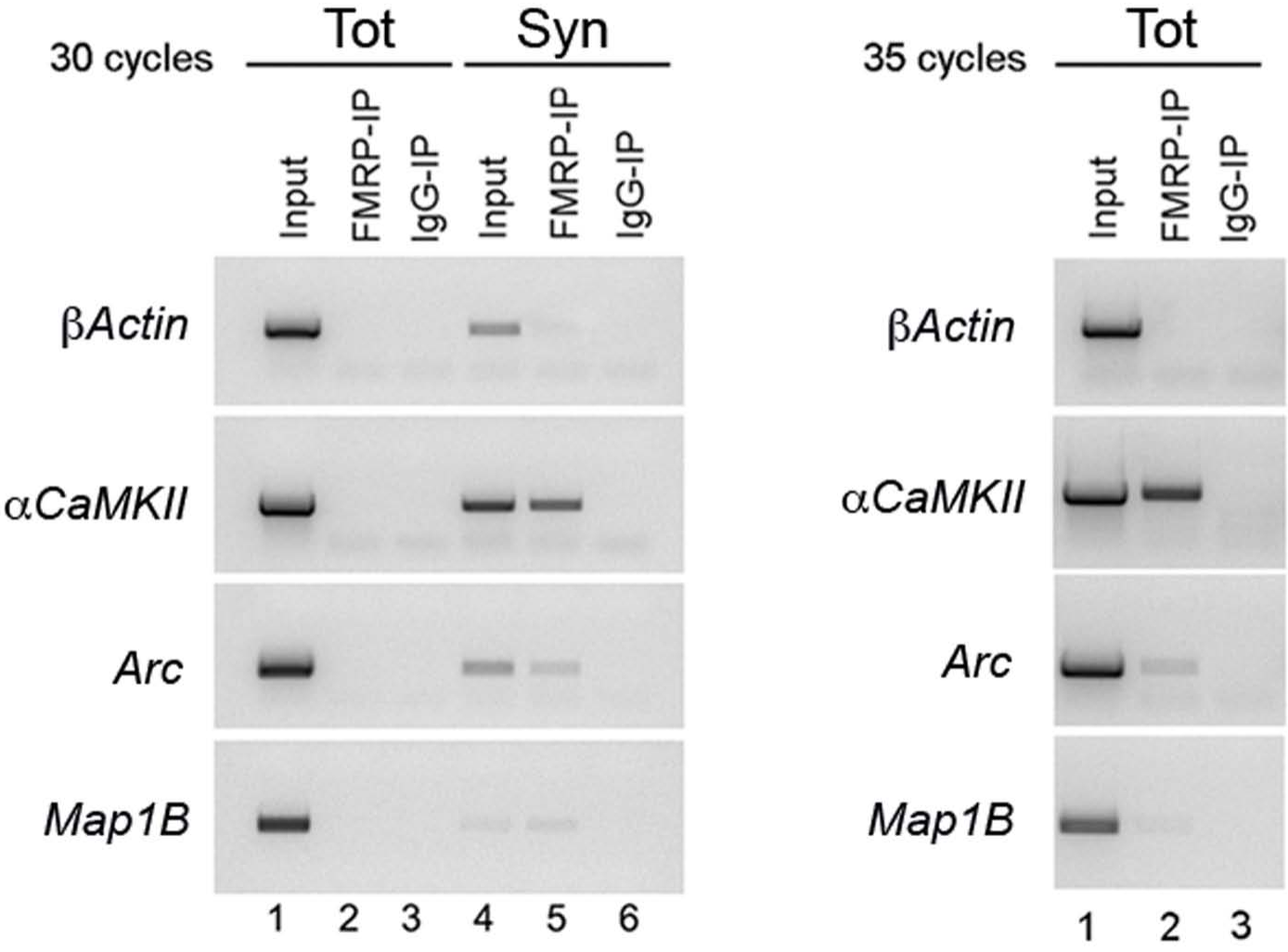

Supplementary Table 1

Hydrogen bond and salt bridge network affecting FMRP-NT and BC1 RNA interaction. Note that not all interactions occur simultaneously in the same modelling solution.

FMRP-NT /unmethylated BC1 RNA		FMRP-NT /G46m/G47m BC1 RNA	
Hydrogen bonds		**Hydrogen bonds**	
Donor	Acceptor	Donor	Acceptor
R70 >NE	A48>5'O	/	/
R70 >NH2	A49>5'O	/	/
Y103>N	G46>4'O	/	/
Y103>N	C45>2'O	/	/
N104>ND2	C32>4'O	/	/
N104>ND2	G31>2'O	/	/
R111>NH1	C47>2'O	/	/
R111>NH1	A48>3'O	/	/
G31>N2	Y103>O	G31>N2	Y103>O
G31>N2	N104>O	G31>N2	N104>O
G46>N2	N104>O	G46>N2	N104>O
Electrostatic interactions		**Electrostatic interactions**	
R70-pA48		/	
R111-pA48		/	
R111-pC47		/	